

A simple analytical model for an elasto-hydrostatic thrust bearing

T Cicone¹, A A Marinescu¹ and S Sorohan¹

¹University POLITEHNICA of Bucharest, Splaiul Independenței 313, Bucharest 060042, Romania

Abstract. A new design of an elasto-hydrostatic bearing with a structurally elastic pad is theoretically analyzed. A single recess circular thrust bearing has the upper pad provided with a large cavity, covered with an elastic metallic membrane. The latter deflects under the pressure distribution in the bearing, creating a radial convergent gap. A simplified axi-symmetric analytical model based on two assumptions is proposed: (i) parabolic approximation for the elastic component of the film thickness and (ii) the maximum elastic deformation of the membrane is calculated analytically using a simplified linear pressure variation in radial direction on the land. Thus, the coupled equations for fluid film and elastic deformation can be solved successively and the bearing performance characteristics can be easily calculated. A parametric analysis, function of a complex elastic parameter and relative recess radius was performed, showing higher load capacity and lower friction similarly to what was previously obtained using rubber-based compliant bearings. A first stage of validation of the analytical model consisted in using a structural finite element model. For the sake of simplicity, the pressure distribution was written in an APDL code using the ANSYS program. The comparison showed small differences for typical values of the recess radius.

1. Introduction

Since the dawn of hydrostatic (HS) bearing applications, the elasticity of one of the mating pads was viewed as a feasible solution for heavy loaded bearings, providing better adaptability to misalignments. After the successful employment of water-lubricated hydrostatic rubber bearings at the Mile High Stadium in Denver, Dowson and Taylor [1], and Castelli et al. [2] published experimental and theoretical studies which proved an increased load carrying capacity and reduced friction when one of the pads was compliant. However, rubber pads inflate at high pressures and cannot be used for a long period of time, due to aging. Moreover, rubber - fluid compatibility may be a major concern. The present paper focuses on a new possible design solution of a HS bearing with a structurally elastic pad. Similar design solutions have been proposed for gas bearings by Hayashi and Hirasata [3] and Hao et al. [4]. Both papers included numerical solutions of the fluid - structure interaction, which showed an improved stiffness. However, the generality of the results was limited to studying only several practical cases. The present work proposes a simplified analytical solution for the coupled fluid film - elastic deformation mechanism, based on an approximate elastic deformation of the elastic pad. The proposed solution allows a quick and comprehensive parametric analysis which reveals the improved performance characteristics of this new design of a compliant HS thrust bearing.



2. The analytical model

The model of the proposed compliant hydrostatic (HS) bearing is shown in figure 1. A classical, axisymmetric, single recess, hydrostatic thrust bearing has a modified, deformable upper pad. A thin shell plate is placed over the upper pad, provided with a large recess of reduced depth. Thus, the plate can be deflected inside the pad under the action of the pressure generated in the bearing. The plate is bent over the extremely thin, outer ridge of the pad, and glued on the outer diameter. The lower pad is assumed rigid and concentric with the upper pad. At rest, the undeformed flexible plate is parallel with the mating face of the lower pad. The lubricant is supplied with pressure p_s into the centrally placed recess of radius r_s , cut into the lower pad; thus, axisymmetry prevails.

For the *fluid flow model*, classical assumptions of HS lubrication theory are used:

- the lubricant is Newtonian and incompressible;
- the flow is laminar and isoviscous, with no slip;
- pressure variation across the film thickness is neglected;
- inertia, gravitational and external forces are neglected.

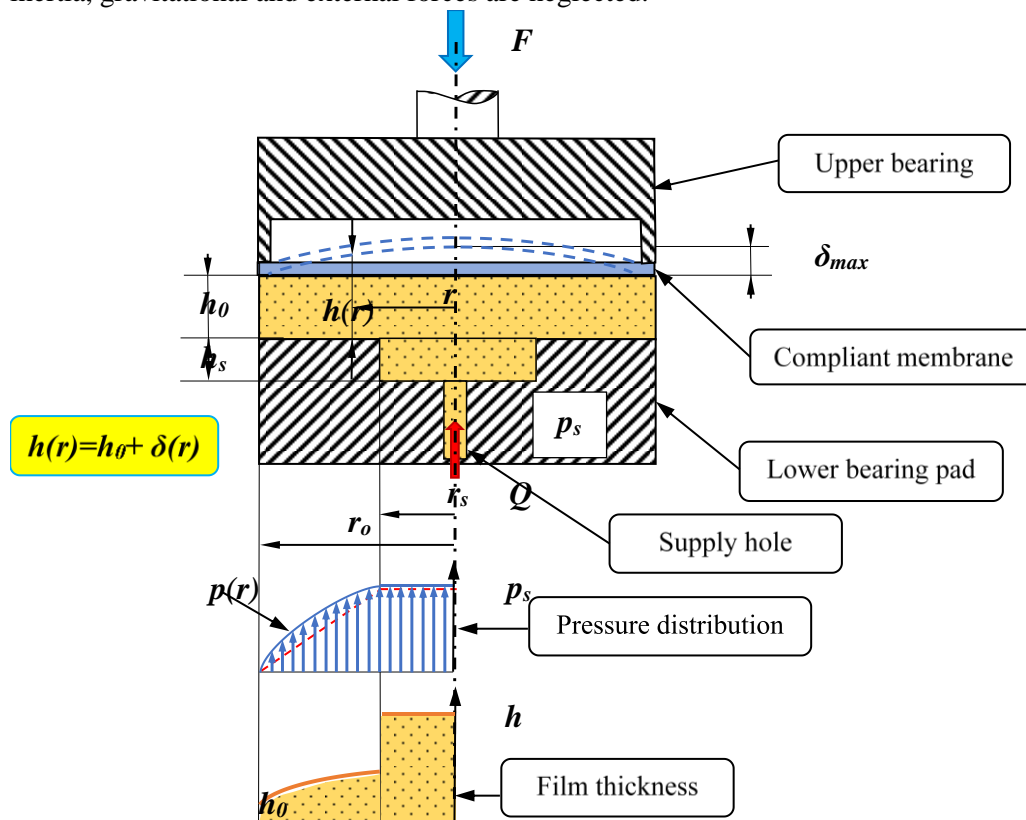


Figure 1. Schematic of the compliant bearing, including pressure distribution and film thickness variation

For the *elastic model*, classical assumptions of plane, plate theory are satisfied:

- the circular plate is perfectly flat, with a uniform thickness much smaller than the bearing radius;
- the material is homogenous and isotropic;
- deformations in the normal plane with respect to the surface of the plate are considerably smaller than the thickness of the plate.

To compute the bearing performance characteristics, the coupled equations for fluid flow and elastic deformations must be solved simultaneously.

According to the above-mentioned assumptions, the Reynolds equation takes the following simplified form for an axi-symmetric hydrostatic thrust bearing with a centrally placed recess:

$$\frac{d}{dr} \left(r h^3 \frac{dp}{dr} \right) = 0 \quad (1)$$

Equation (1) can be solved in order to obtain the pressure distribution, only if the film thickness is defined. Thus, for the HS bearing, film thickness can be expressed as follows:

$$h(r) = h_0 + h_{el}(r) \quad (2)$$

where h_0 is the minimum film thickness (at the outer boundary of the bearing), and h_{el} is the elastic deformation of the upper plate of the bearing, produced by the pressure distribution. The latter can be calculated from general equations of elasticity for the pressure distribution obtained after solving the Reynolds equation.

A solution of this system of equations can be obtained only by using an iterative numerical procedure. Such a procedure does not facilitate parametric investigations; as consequence, a simplified approach is proposed, based on supplementary assumptions, which allow uncoupling the two mechanisms.

A parabolic variation of the elastic component of the film thickness is assumed along the radial direction of the bearing, with a maximum value, δ_{max} , in the centre axis of the bearing:

$$h_{el} = \delta_{max} \left[1 - \left(\frac{r}{r_o} \right)^2 \right] \quad (3)$$

Further, the maximum deflection of the thin plate is calculated analytically, using a simplified pressure distribution in the bearing. Because the depth of the recess is much greater than the film thickness, the pressure distribution is assumed constant in the recess and drops down to a value corresponding to the outer atmospheric pressure (null relative pressure) following an inflated curve. A schematic of this pressure variation is shown in figure 1. The two model components will be further described in detail.

2.1 Elastic plate model

Due to the complex shape of the compliant upper plate, the deformation produced by the real pressure distribution cannot be calculated analytically. The proposed model follows a simplified approach based on the well-known plane plate theory, which considers a flat plate of uniform thickness, made of a homogeneous and isotropic material. The elastic deformation of the upper plate is analytically calculated for a simplified pressure distribution in the bearing, with linear variation on the land. Analytical solutions of the elastic deformation in plane circular plates, simply supported on the outer edge and axi-symmetrically loaded with either constant pressure or linearly variable pressure, can be found in [5]. The elastic component of the film thickness defined as a function of the maximum deflection is briefly reproduced herein, in dimensionless form.

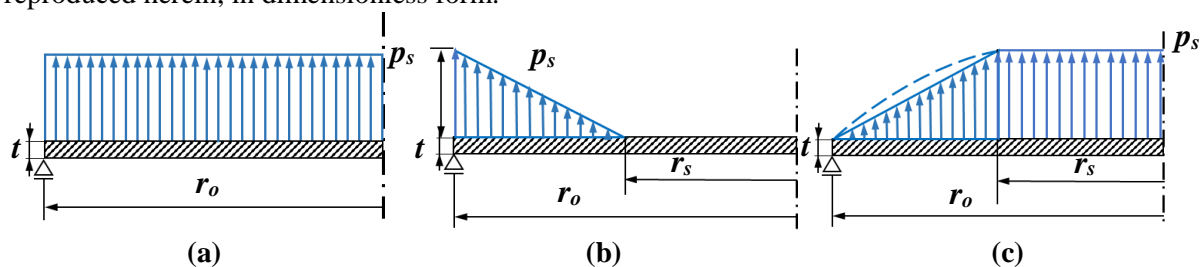


Figure 2. Simplified load cases for the elastic model

(a): constant pressure distribution on the entire plate (figure 2a)

$$\bar{\delta}_{\max_1} = K_e \frac{3}{16} (5 + \nu)(1 - \nu) \quad (4)$$

(b): linear pressure distribution on an annular surface (figure 2b)

$$\bar{\delta}_{\max_2} = 6K_e [(1 - \nu)L_1 - 2(1 - \nu^2)L_2] \quad (5)$$

where $\bar{\delta}_{\max} = \frac{\delta_{\max}}{h_0}$ and

$$L_1 = \frac{1}{720(1 - R)} [(20R^3 + 16)(4 + \nu) - 45R(3 + \nu) - 9R^5(1 - \nu) - 60R^3(1 + \nu)\ln R] \quad (6)$$

$$L_2 = \frac{1}{14400(1 - R)} [64 - 225R - 100R^3 + 261R^5 - 60R^3(3R^2 + 10)\ln R] \quad (7)$$

From equations (4) – (7) one can remark that the dimensionless form of the maximum deformation is expressed in terms of two important parameters: $K_e = \frac{p_s r_o^4}{Et^3 h_0}$ is a complex elastic parameter (which depends on the geometry and material properties of the elastic membrane), and $R = \frac{r_s}{r_o}$ is the relative recess radius.

Finally, for the simplified pressure distribution in the bearing (figure 2c), one can obtain the maximum deflection in dimensionless form, based on superposition of effects:

$$\bar{\delta}_{\max} = \bar{\delta}_{\max_1} - \bar{\delta}_{\max_2} = K_e \left[\frac{3}{16} (1 - \nu)(5 + \nu) - 6(1 - \nu)L_1 + 12(1 - \nu^2)L_2 \right] \quad (8)$$

2.2 Fluid flow model

Using dimensionless notations, the Reynolds equation (1) becomes

$$\frac{d}{d\bar{r}} \left(\bar{r} \bar{h}^3 \frac{d\bar{p}}{d\bar{r}} \right) = 0 \quad (9)$$

and film thickness can be written as:

$$h(\bar{r}) = 1 + \bar{\delta}_{\max}(1 - \bar{r}^2) \quad (10)$$

Considering the classical boundary conditions for pressure in single recess circular bearings ($\bar{p} = 1$ at $\bar{r} = R$ and $\bar{p} = 0$ at $\bar{r} = 1$), after integration and several algebraic manipulations, one can obtain the pressure distribution on the land:

$$\bar{p}(\bar{r}) = \frac{\left[\frac{3\Delta^2 - 2\Delta\bar{r}^2}{(\Delta - \bar{r}^2)^2} - \frac{\Delta(3\Delta - 2)}{(\Delta - 1)^2} + 2\ln\left(\bar{r}^2 \frac{\Delta - 1}{\Delta - \bar{r}^2}\right) \right]}{\left[\frac{3\Delta^2 - 2\Delta R^2}{(\Delta - R^2)^2} - \frac{\Delta(3\Delta - 2)}{(\Delta - 1)^2} + 2\ln\left(R^2 \frac{\Delta - 1}{\Delta - R^2}\right) \right]} \quad (11)$$

where $\bar{p} = \frac{p}{p_s}$, and $\Delta = 1 + \frac{1}{\bar{\delta}_{\max}}$ is a dimensionless elastic parameter used to compact the equation.

Figure 3 shows the inflated pressure distribution for a bearing with the recess radius half the outer radius ($R = 0.5$), for different values of the elasticity parameter, K_e .

It is worth noting that for a rigid bearing, $\Delta \rightarrow \infty$ and equation (11) yields to the classical formula for rigid bearings:

$$\bar{p}(\bar{r}) = \frac{\ln \bar{r}}{\ln R} \quad (12)$$

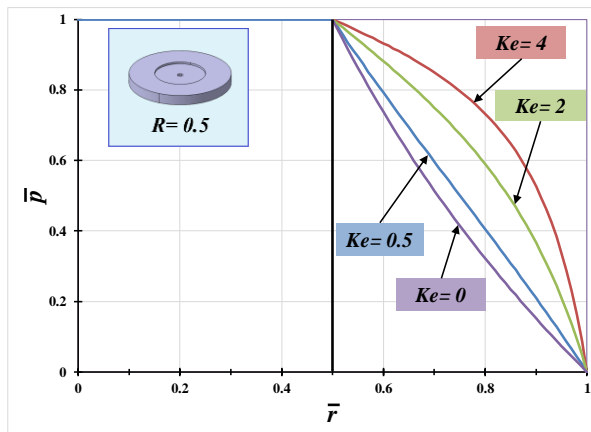


Figure 3. Dimensionless pressure distribution

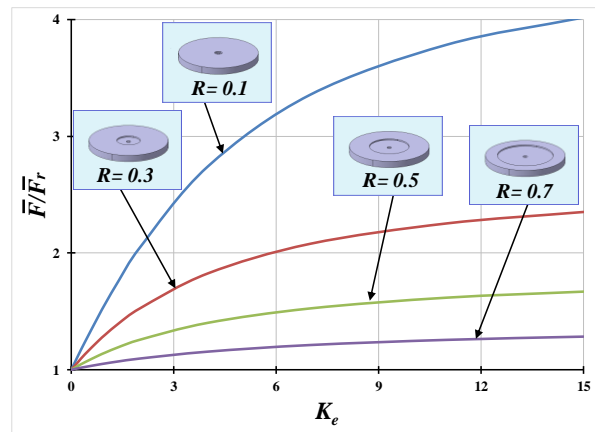


Figure 4. Relative load carrying capacity

The load carrying capacity can be obtained only by integrating numerically the pressure distribution:

$$\bar{F} = \frac{F}{\pi r_o^2 p_s} = R^2 + 2 \int_R^1 \bar{r} \bar{p} d\bar{r} \quad (13)$$

The beneficial effect of elasticity, for various sizes of the recess, is clearly depicted in figure 4 in terms of the ratio between the actual load carrying capacity and that of the rigid bearing $\bar{F}_r = \frac{1-R^2}{2 \ln \frac{1}{R}}$. The greater the elasticity parameter, the greater the load capacity; however, the elasticity parameter is limited by the high stresses in the plate.

The rate of flow results after differentiating the pressure distribution:

$$\bar{Q} = Q \frac{\eta}{p_s h_0^3} = -\frac{2\pi}{3} \cdot \frac{\left(\frac{\Delta}{\Delta-1}\right)^3}{\frac{3\Delta^2 - 2\Delta R^2}{(\Delta - R^2)^2} - \frac{\Delta(3\Delta - 2)}{(\Delta - 1)^2} + 2 \ln \left(R^2 \frac{\Delta - 1}{\Delta - R^2}\right)} \quad (14)$$

The predicted values divided by the rate of flow of the rigid bearing ($\bar{Q}_r = \frac{\pi}{6 \ln R}$), for different sizes of the recess, are shown in figure 5.

The friction torque for rotational speed ω and lubricant dynamic viscosity η , yields:

$$\bar{M}_f = M_f \frac{h_0}{\eta \omega r_o^4} = 2\pi \int_R^1 \frac{\bar{r}^3}{a - b\bar{r}^2} d\bar{r} = \pi(\Delta - 1) \left[(R^2 - 1) + \Delta \ln \left(\frac{\Delta - R^2}{\Delta - 1} \right) \right] \quad (15)$$

Figure 6 presents the values of the friction torque divided by the friction torque of the rigid bearing $\bar{M}_{fr} = \frac{\pi}{2}(1 - R^4)$.

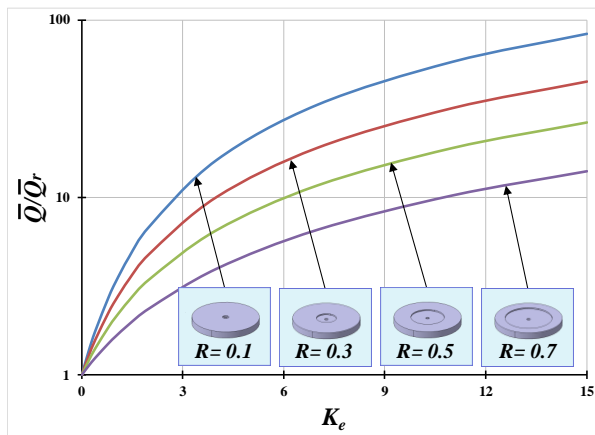


Figure 5. Relative rate of flow

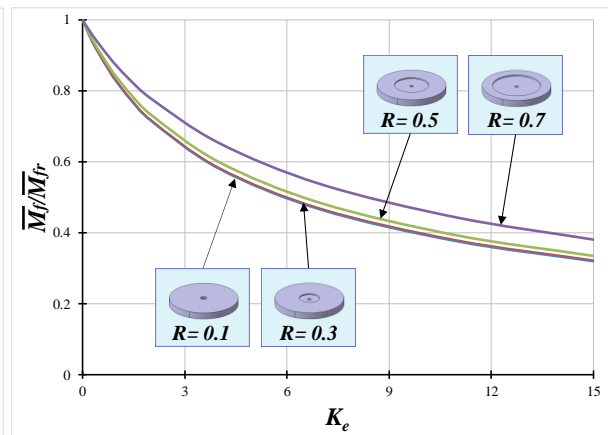


Figure 6. Relative friction torque

3. The FE model

The accuracy of the proposed analytical model of the elastic plate was evaluated using structural FE simulation. This approach uses a particular design solution of the elastic membrane ($r_o=50\text{mm}$, $t=3\text{mm}$), made of steel ($E=210\text{GPa}$ and $\nu=0.3$) which is meshed with regular quadrilaterals (element type - PLANE183 axi-symmetric). A total number of 5217 nodes and 1600 elements was found sufficient for yielding a reasonable accuracy, due to the fact that the model did not include an intricate geometry. The boundary conditions were identical with the ones considered for the simplified analytical model, whereas the pressure distribution applied on the bottom side of the membrane was computed using the analytical model - equation (11). Two representative sizes of the recess radius were considered, and the results were compared with the analytically predicted values, calculated with the maximum plate deformation, obtained two load cases. For load case 1 (figure 2c) the maximum deformation is calculated with equation (8) and slightly underestimates the real load distribution, whilst for load case 2 (figure 2a) the deformation is calculated with equation (4), yielding to an overestimated solution.

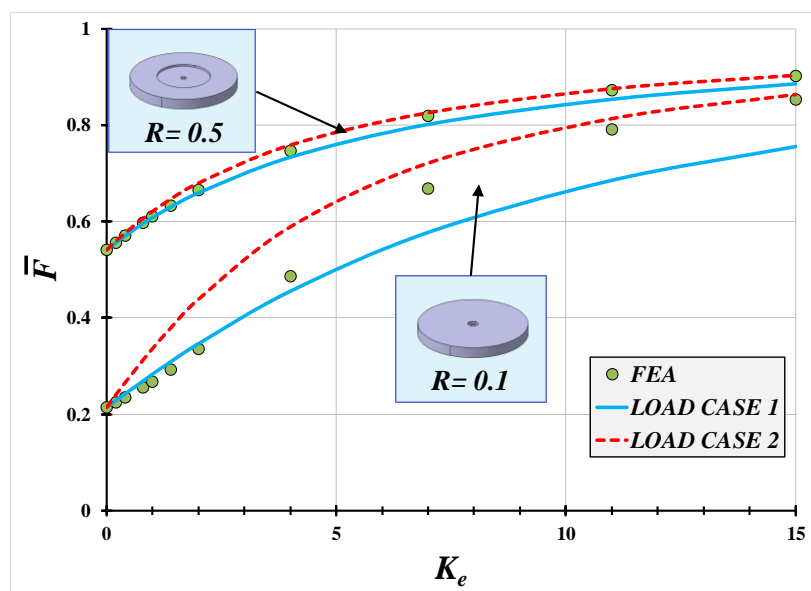


Figure 7. Analytical vs. FEA load capacity

Figure 7 represents the most valuable result of the present work. The graph depicts the load carrying capacity predicted theoretically using two models for the pressure distribution of the elastic plate (constant pressure and combined pressure, respectively), and results obtained used pseudo-numerical FE model. One can observe that, for values of $K_e < 5$, it is more accurate to use the combined load case 1, whilst for values of $K_e > 5$, a constant pressure load case 2, approximates better the elastic behaviour.

4. Conclusions

An original design solution of a compliant hydrostatic bearing is theoretically analysed. Based on simplified pressure distribution and elastic deformation, analytical formulations for bearing performance characteristics are proposed. The predicted results are shown relatively to those obtained for the rigid bearing. The superior load capacity and lower friction torque of the elastic HS bearing are put in evidence with the proposed model. The accuracy of the elastic component of the model has been evaluated by finite element analysis (FEA) and a two-range analytical formulation was proposed. The limits of elasticity due to high stresses are also defined using FEA. A coupled numerical approach for more accurate solutions of bearing performances is foreseen for the next step of the analysis.

5. References

- [1] Castelli V, Rightmire G K and Fuller D D 1967 On the analytical and experimental investigation of a hydrostatic, axisymmetric compliant-surface thrust bearing *ASME J. Lubr. Technol.* **89(4)** 510-519
- [2] Dowson D and Taylor C M 1967 Elastohydrostatic lubrication of circular plate thrust bearings *ASME J. Lubr. Technol.* **89(3)** 237-242
- [3] Hao D, Xiao-Long Z and Juan-An Z 2015 Static characteristic analysis and experimental research of aerostatic thrust bearing with annular elastic uniform pressure plate *Advances in mechanical engineering* 1-13
- [4] Hayashi K and Hirasata K 1982 Theoretical Investigation on the back-pressured elastohydrostatic thrust bearing *Journal of JSLE International Edition* **3(3)** 277-283
- [5] Young W and Budynas R 2011 *Roark's Formulas for Stress and Strain* McGraw-Hill 7th Edition New York